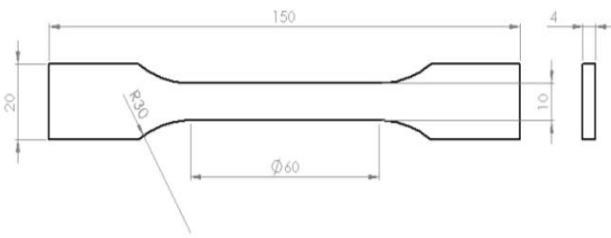
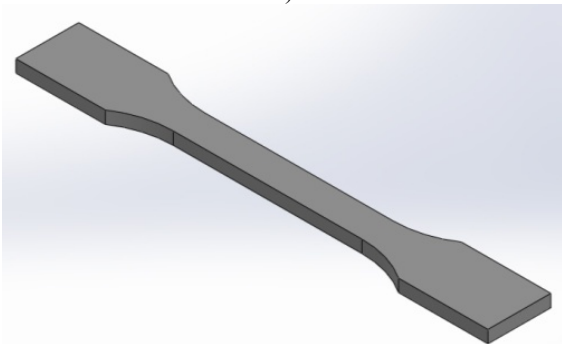


Fig.2. Standard graph [2], [3]

The landmark used for experimental research is a specimen obtained under STAS DIN EN ISO 527-1: 1993, through injection procedure using as material the polyamide 6.6, being presented in figure 3 [4].



a)



b)

Fig. 3. Specimen DIN EN ISO 527+1: 1993; a) 2D drawing, b) 3D drawing

## 2. EXPERIMENT PREPARATION AND THE SIMULATION RESULTS

In table 2 are presented the variation levels for the input parameters for polyamide 6.6 nature.

Table 2. The variation levels of the input parameters for polyamide 6.6 nature.

| Input parameter | $T_{top}$ [°C] | $t_{inj}$ [s] | $t_r$ [s] | $V_{inj}$ [m/min] | $P_{inj}$ [MPa]Kgf | $T_{mat}$ [°C] |
|-----------------|----------------|---------------|-----------|-------------------|--------------------|----------------|
| Levels          |                |               |           |                   |                    |                |
| Level 1         | 220            | 10            | 4         | 30                | 70                 | 40             |
| Level 2         | 250            | 15            | 10        | 50                | 90                 | 70             |

This analysis studies the process of filling the mold cavity using the finite element method. Simulation programs allow you to view how the cavity is filling and highlighting where mechanical strength is low, air inclusions, mold release, etc. The parameters used for setting simulation are shown in Table 2, for polyamide 6.6 Nature and their values are suitable with experiment 1 of Table 1.

### 2.1 The results obtained from simulation

The simulated data are presented in Table 3.

Table 3. Simulation results at flowing

|                                 |                |
|---------------------------------|----------------|
| Closing force on direction X    | 2.790 Tone     |
| Closing force on direction Y    | 5.320 Tone     |
| Closing force on direction Z    | 1.140 Tone     |
| Injection pressure              | 70 Mpa         |
| Maximum temperature of the melt | 220.260 °C     |
| Average temperature of the melt | 199.630 °C     |
| Maximum shear tension           | 0.260 Mpa      |
| Maximum shear rate              | 1737.270 1/sec |
| Cooling time                    | 3 sec          |

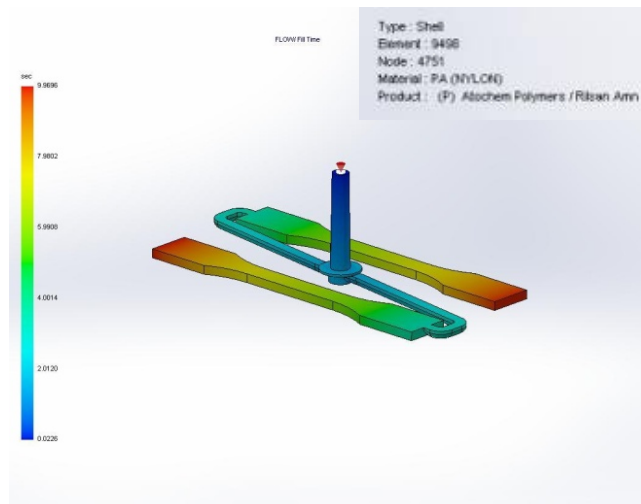


Fig. 4. Variation of filling time

In Figure 4 is presented the melt flow position at certain intervals. Blue regions represents the beginning of the cavity filling process and red regions represents the complete filling area of the cavity in a preset time by the experimental plan.

Atmospheric pressure is defined as the ratio of normal force and unit area. In injection process, the injection force, given by the screw or by the piston from the injection cylinder, is used for pushing molten material inside the cavity. The injection force propagates through the melt resulting a distribution of

pressures inside the cavity, as is shown in Figure 5. The red area shows high levels of injection pressure, respectively, low pressure in the blue area. As it can be seen, the pressure distribution at the end of the injection has high values in the injection and low on the most remote areas because it have to maintain a constant flow of melt and the contact area of the melt with the cavity is increasing. In the case of thin-walled parts pressures grow a lot more because during the filling process solidification phenomenon occurs which leads to increased resistance to filling.

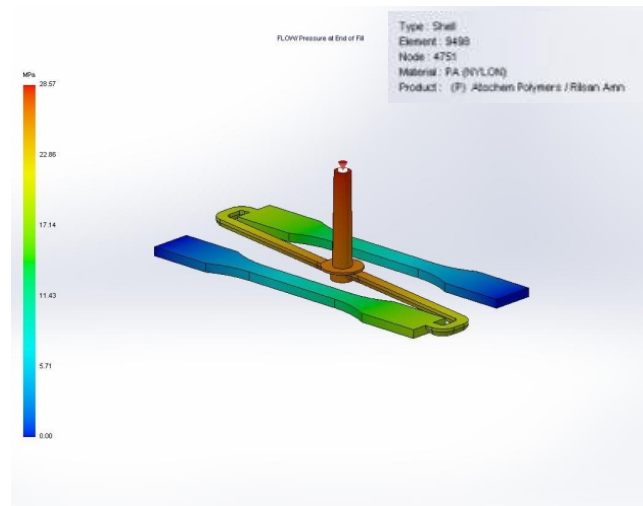


Fig. 5. The end of injection pressure

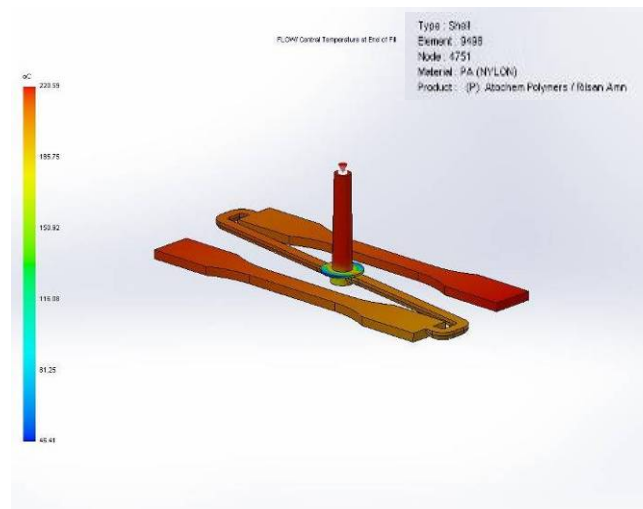


Fig. 6. The central temperature at the end of filling

Figure 6 shows the central temperature at the end of cavity filling period and is defined as the highest temperature inside the cavity, being located at the farthest distance from cavity walls. This temperature can have a sudden drop in areas where injected marker wall has very thin walls (the end area of the abutment). The red area represents the area with the highest temperatures, while in the blue area are the lowest temperature values. Figure 7 shows a distribution of the average temperature from the surface of the cavity walls, significance of chromatics

being identical to that from the central temperature distribution shown in Figure 6.

An uneven sharp of the average temperature distribution leads to the production of very large deformations /contractions of the injected marker.

The volume melt temperature variation is shown in Figure 8 and represents the average temperature of the melt, in motion, between cavity walls all over it. If the speed of the melt movement is zero, the temperature of the melt volume is equal to the average temperature.

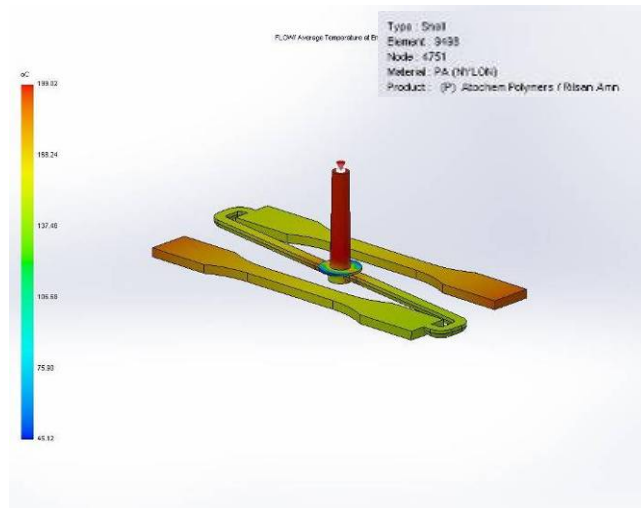


Fig. 7. The average temperature of the melt

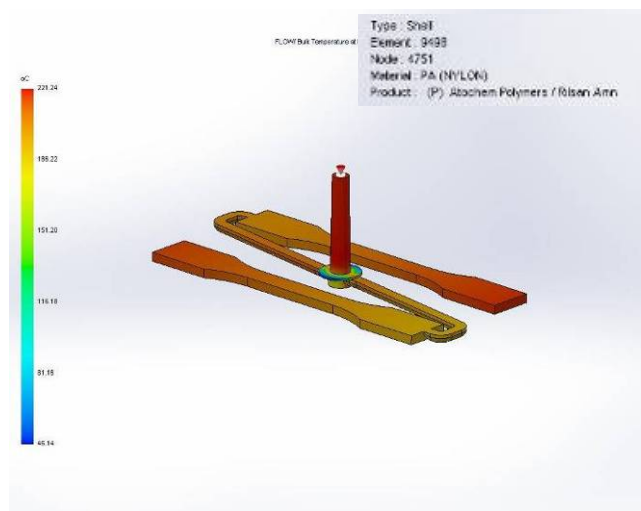


Fig. 8. The temperature of the melt volume

Generally the temperature is highest in areas where the melt flow rate is high. This distribution can provide information about the areas in which the polymer heats in excess and could result the degradation phenomenon.

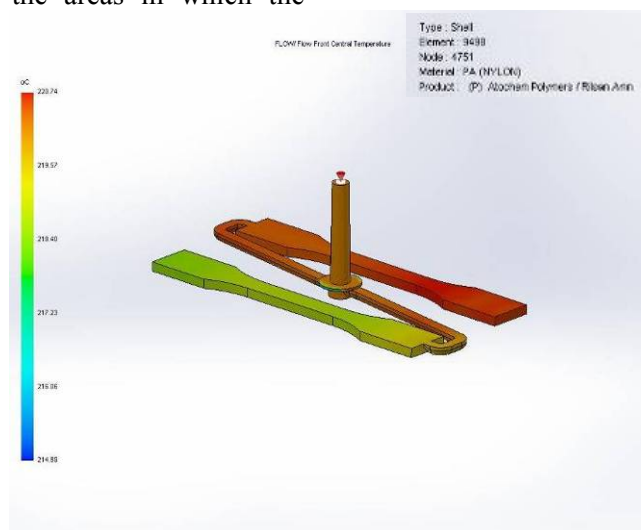


Fig. 9. Melt flow temperature

Melt flow temperature represents the temperature from the front area of the molten polymer flow in the central area, as shown in Figure 10. Melt flow temperature variation is shown in Figure 9, and the significance of chromatics is the same as that shown in the temperature variation graphs.

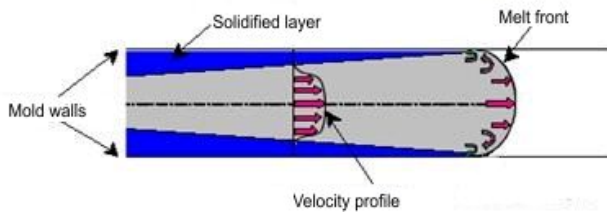


Fig. 10. Polymer melt flow

During the injection, the polymer is subjected to additional heating due to the shearing which can lead to an increase in its temperature higher than the melting temperature. Prin simulation may determine the increase of this temperature and is recommended to not exceed a maximum value from 30 ° C. In this case (figure 11) thevalue of this temperature is 1.09 ° C in the abutment.

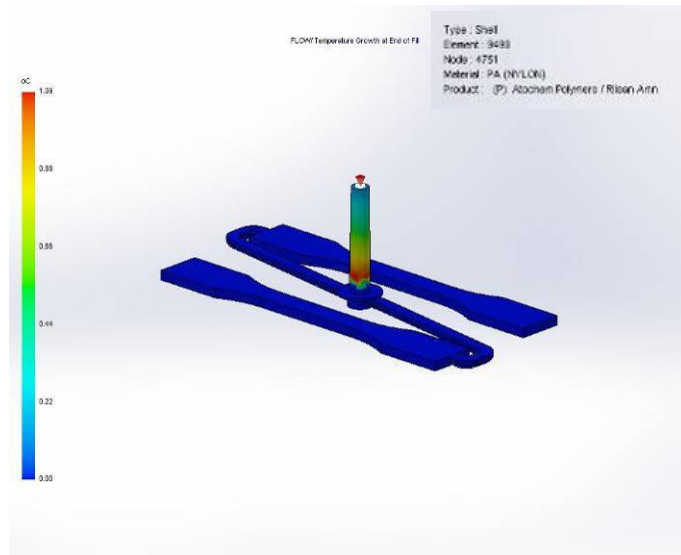


Fig. 11. The rise of temperature after filling

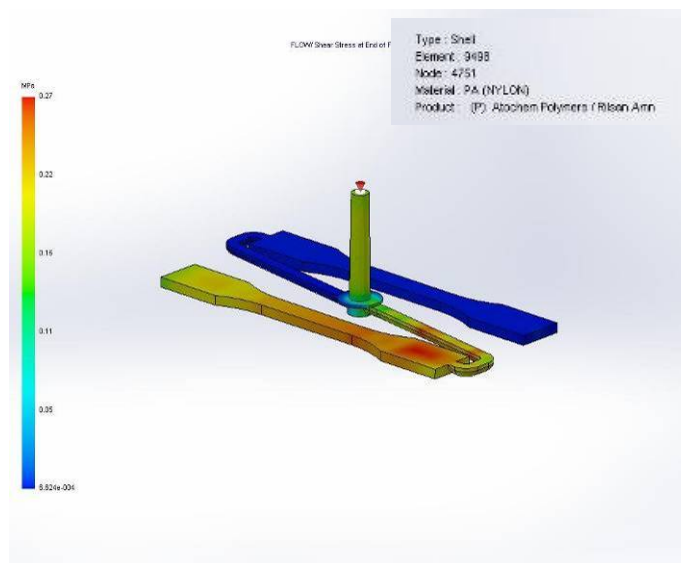


Fig. 12. The shearing tension

The shearing tension is defined as the shearing force per unit area. A large value of the shearing tension that appears between the cavity wall and the melt may cause the increasing of the internal pressure and of the surfaces with high roughness.

In Figure 12 is shown the distribution of the shearing tension when filling the cavity on a single nest, because the mark is symmetrical. The maximum value of the shearing tension resulting from

simulation is 0.23 MPa, and the admissible value of polyamide is 0.31 MPa and is found in areas marked in red on the work. The shearing rate shown in Figure 13 is defined as the modification of the shearing tension in unit time. Following the simulation, the maximum value of the shearing rate is 1119. 089 1/sec and is presented in the red area.

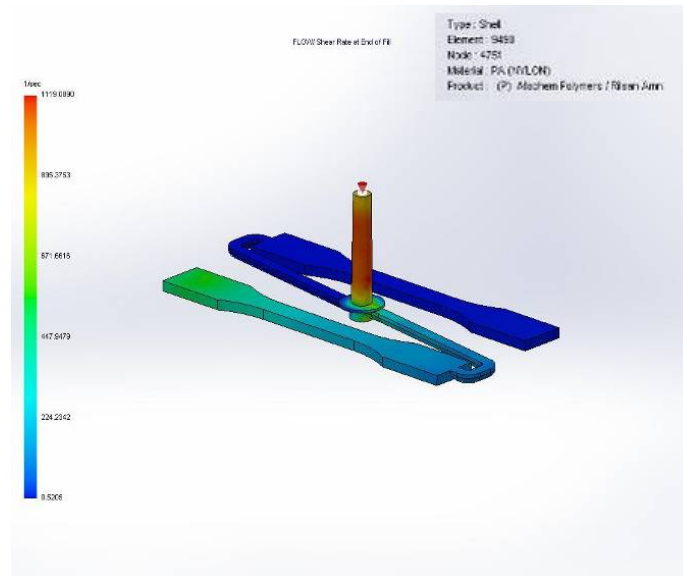


Fig. 13. The shearing rate

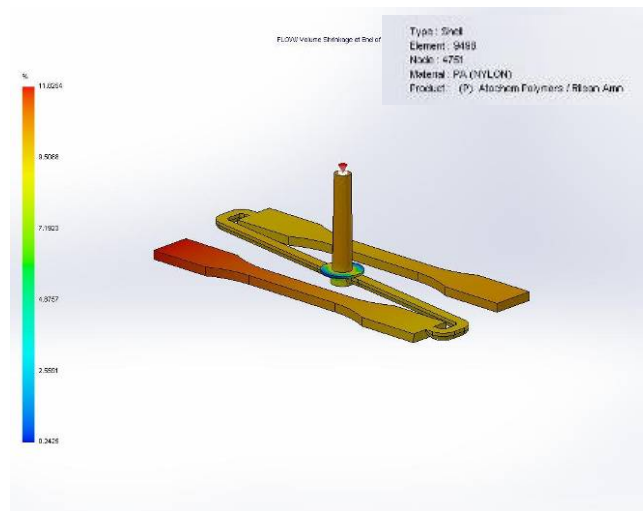


Fig. 14. Volume contraction

Volume contraction variation from Figure 14 has a maximum value of 11.8254% and is the phenomenon that appears when the workpiece cools to ambient temperature after removal from the mold.

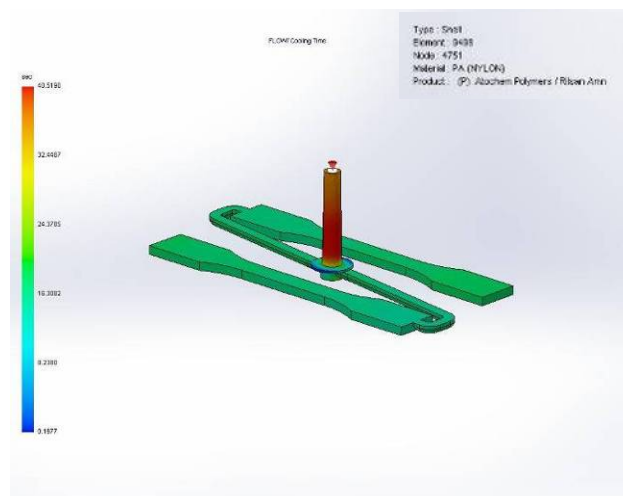


Fig. 15. Cooling time

Cooling time variation is presented in figure 15, the maximum value being 40.51 s and is found in the abutment area.

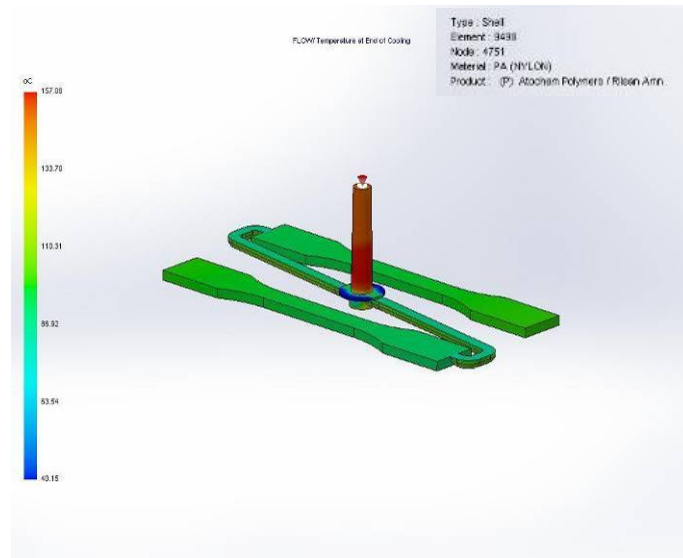


Fig. 16. The proper temperature for end filling

Figure 16 presents the workpiece variation temperature after complete filling of the mold cavity.

The maximum amount obtained from simulation is 157.08°C.

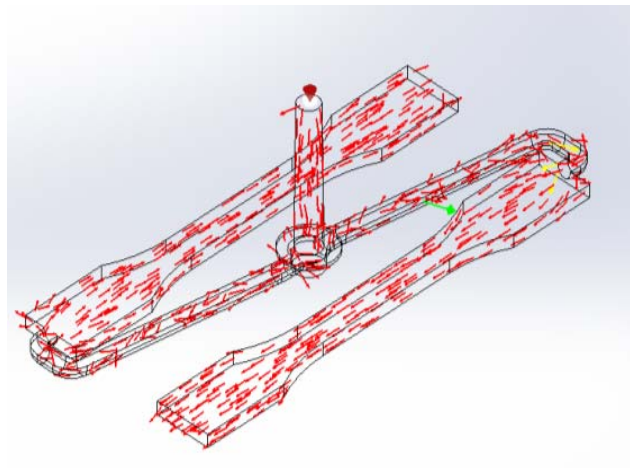


Fig. 17. Fiber orientation

In Figure 17 we can see the fiber orientation and distribution. In Tables 4 and 5 are presented the simulation results to compaction and bending.

Table 4. Simulation results in compaction

|                          |              |
|--------------------------|--------------|
| Maximum temperature      | 217.710 °C   |
| Average temperature      | 170.140 °C   |
| Maximum shearing tension | 0.670 Mpa    |
| Maximum shearing rate    | 2.5559 1/sec |
| Residual tension         | 97.220 Mpa   |

Table 5. Simulation results in bending

|                                 |                     |
|---------------------------------|---------------------|
| Displacement in the X direction | 0.1688 mm (Fig. 18) |
| Displacement in the Y direction | 0.5745 mm (Fig. 19) |
| Displacement in the Z direction | 0.9546 mm (Fig. 20) |
| Total displacement              | 1.1204 mm (Fig. 21) |

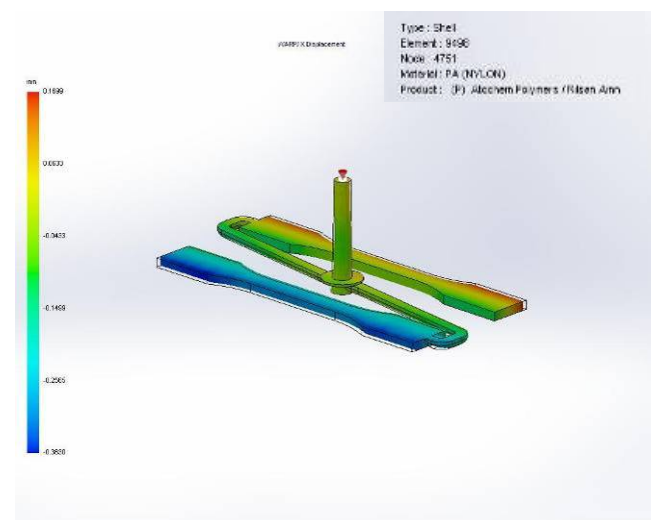


Fig. 18. Displacement in the X direction

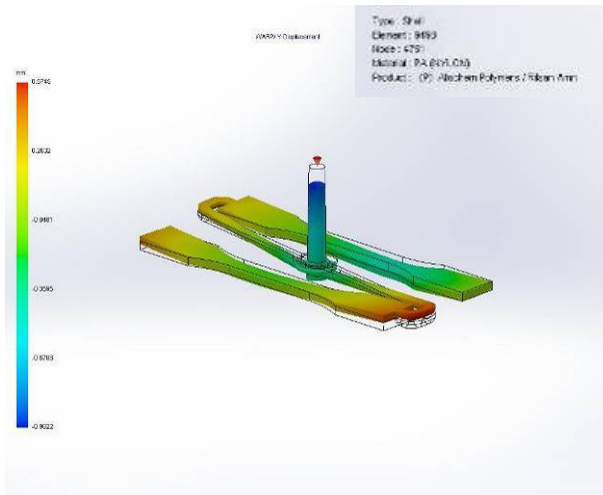


Fig. 19. Displacement in the Y direction

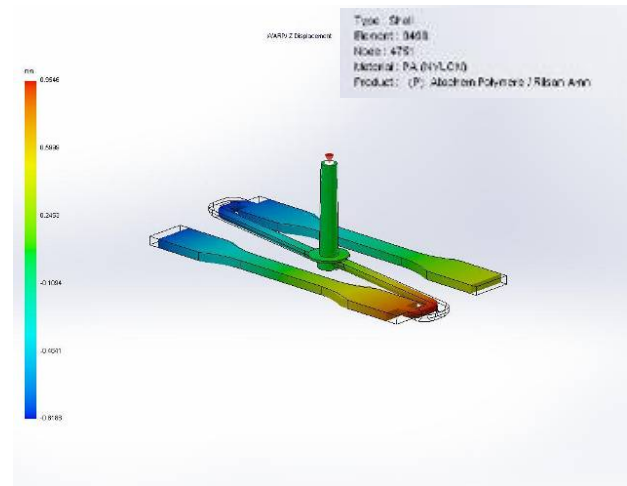


Fig. 20. Displacement in the Z direction

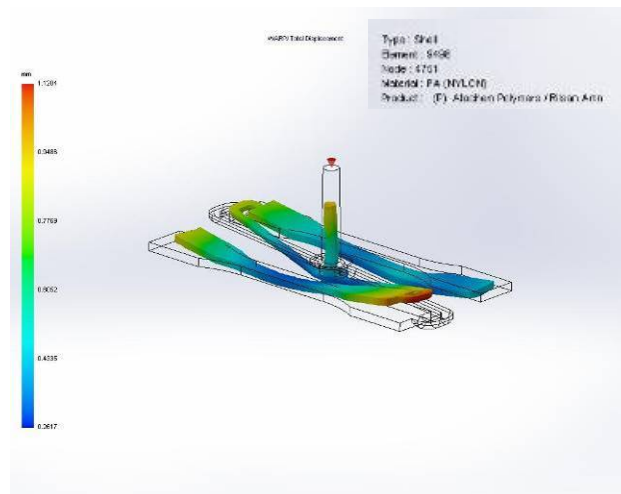


Fig. 21. Total displacement

### 3. CONCLUSIONS

Using a Taguchi experimental plan, leads to a reduction in the number of experiments to be performed, without a major influence on the experimental results obtained. Following the rapid development of polymeric materials processing it can be seen the appearance and the development of some software tools that provide high accuracy results, with the aim to facilitate the work of designers and to reduce the time of calculations. Also due to the virtual environment simulation are significantly reduced the number of physical prototypes, leading to lower production costs.

Finite element analysis allows, besides studying injection process in virtual environment and an optimization, offering the possibility of balancing the nest filling, to change the fibers orientation by changing the point of injection, etc. without the need for execution of an injection mold.

A major advantage of using simulation software in the injection of polymeric materials is that it allows detailed study of the phenomena that take place inside the mold during the injection process.

### Acknowledgement

This paper was realised with the support of POSDRU CUANTUMDOC “DOCTORAL STUDIES FOR EUROPEAN PERFORMANCES IN RESEARCH AND INNOVATION” ID79407 project funded by the European Social Fund and Romanian Government.

### 4. REFERENCES

1. Fetecău, C., (2007). *Injectarea materialelor plastice*, Second Edition, EDP Publishing House, ISBN: 978-973-30-1971-8, Bucharest.
2. Nedelcu, D., (2001). *Tehnologii de Mecanica Fina*, Tehnica-Info Publishing House, Chisinau, pp. 238-243.
3. Osswald, T., Lih-Sheng, T. & Gramann, P. (2008). *Injection Molding Handbook*, Hanser Verlag, ISBN: 978-3-446-40781-7, 2nd Edition, Ohio.
4. Șereș, I., (1996). *Injectia materialelor termoplastice*, Imprimeria de Vest Publishing House, ISBN: 973-97652-6-2, Oradea.